## RESEARCH ARTICLE

**Open Access**

# A practical fully automated radiosynthesis of [18F]Flurpiridaz on the module modular lab-pharmtracer without external purification

Kurtulus Eryilmaz and Benan Kilbas*

*Correspondence:
bkilbas@gmail.com

Moltek A. S. Gebze Organize
Sanayi, 41400 Gebze, Kocaeli,
Turkey

## Abstract

**Background:** [18F]Flurpiridaz is a promising novel cardiac PET imaging tracer formed by the radiolabeling of pyridaben derivative with fluorine-18. Clinical studies on [18F]Flurpiridaz are currently at the phase III level for the assessment of MPI. Providing high image quality thanks to its relatively long half-life, F-18 is a high-potential radionuclide for the early detection of CAD. In this study, we aimed to develop a fully automated synthesis of [18F]Flurpiridaz without further preparative HPLC purification.

**Results:** Precursor **6** was obtained by multi-step synthesis starting from mucochloric acid (**1**) as a sole product with 35% yield and identified by spectroscopic measurement. Manually cold labeling experiments were performed using the stable isotope [19F]F, and TBA-HCO$_3$ PTC provided desirable fluorinated compound with high yield. A fully automated [18F]Flurpiridaz synthesis on the ML-PT device provided 55–65% radiochemical yield with more than 98% radiochemical purity. The final product purification method demonstrated that [18F]Flurpiridaz could be obtained without an external preparative HPLC system as a pharmaceutical quality.

**Conclusion:** A novel and fascinating strategy was developed for the fully automated synthesis of [18F]Flurpiridaz (**7**) on ML PT. Organic synthesis of precursor **6** was achieved with a desirable yield and characterized by NMR and HR-MS. A detailed set of cold experiments were completed for optimization conditions before hot trials and TBA-HCO$_3$ increased molar activity with a minimum amount of side products. Radiolabeling showed that our self-designed automated synthesis method enables high radiochemical yield and radiochemical purity for the production of [18F]Flurpiridaz. The desirable radiopharmaceutical quality of the product was obtained without using an additional preparative HPLC system. [18F]Flurpiridaz (**7**) preserved its stability within 12 h and final specifications were consistent with the acceptance criteria in Ph. Eur. regulations.

**Keywords:** Automated synthesis, Cardiac PET, 18F, [18F]Flurpiridaz

## Background

Coronary artery disease (CAD) has been frequently observed worldwide which causes mortality due to the coronary artery atherosclerosis (Fowkes et al. 2017). Increase the number of CAD led to investigations of different treatment approaches (Davidson et al. 2018). Myocardial perfusion imaging (MPI) tools, such as cardiac magnetic resonance
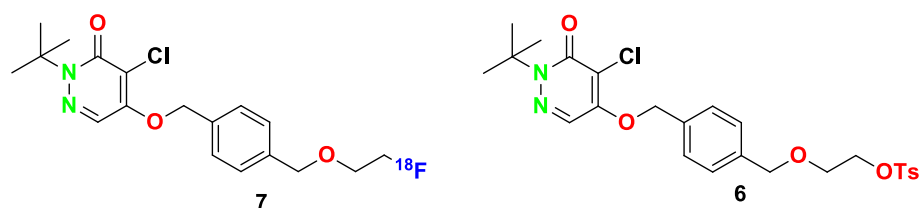
**Scheme 1**  Molecular Structures of [$^{18}$F]Flurpiridaz **(7)** and its precursor **6**

(CMR), single-photon emission computed tomography (SPECT) and positron emission tomography (PET) have for the past decades attracted increasing interest for an accurate diagnosis of coronary heart disease (Danad et al. 2017). [$^{99}$Tc]Tc-Sestamibi, approved agent by FDA is well known SPECT-tracer as a diagnostic agent for clinics. Even though it has been widely used as a diagnostic agent, it has some limitations such as less spatial resolution and additional correction measurement (Wu et al. 2009). Recently, positron emission tomography (PET) has been most widely utilized in MPI due to the better diagnostic performance, high resolution of images and lower radiation exposure (Di Carli et al. 2007). Even though, [$^{82}$Rb]Rb (Huang et al. 1989), [$^{13}$N]N (Schelbert et al. 1981), [$^{11}$C]C (Croteau et al. 2012), and [$^{15}$O]O (Bergmann et al. 1989) have been exhibited as PET radionuclides for the detection of MPI, shorter half-life and higher cost cause a limit of their widespread use. For example, [$^{82}$Rb]Rb generator is replaced every one month with a high amount of cost (€ 30.000 per one month). Recently, [$^{68}$Ga]Ga-DOTA has been exhibited as an alternative PET agent for MPI in small animals however comprehensive clinical trials are necessary to be a reliable diagnostic agent (Autio et al. 2020). Those limitations of available PET tracers have led to a need for an optimal perfusion agent with improved properties. [$^{18}$F]Flurpiridaz is an ideal pyridaben-derivative $^{18}$F-labeled MPI agent which binds to mitochondrial complex (MC) I inhibitor with high affinity (Scheme 1) (Maddahi et al. 2020). Preclinical and clinical trials have indicated that [$^{18}$F]Flurpiridaz is clinically safe and enhances a high-resolution quality of image and particularly it is more favorable in women, obese patients and patients with multivessel disease. (Berman et al. 2013) Besides, one cyclotron site can be sufficient for dose distribution to many different nuclear medicine centers due to the relatively long physical half-life feature of Fluorine-18.

To the best our knowledge, detailed radiolabeling study of [$^{18}$F]Flurpiridaz **(7)** has not been published yet despite expected popularity of its use in many clinics. In this article, the scope was to demonstrate a fully automated synthesis of [$^{18}$F]Flurpiridaz **(7)** radiopharmaceutical considering radiation safety and in accordance with regulations of radiopharmaceutical preparations by using commercially available an automated synthesis platform namely Modular Lab-PharmTracer (ML PT) for the first time.

## Methods

### Materials
Chemicals and solvents were supplied from Sigma-Aldrich (Germany) and directly used without any further purification. Reactions were magnetically stirred and monitoring was determined by TLC performed on Merck TLC plates (silica gel 60 F254). The resulting TLC spots were detected with UV light ($\lambda = 254$ nm and 360 nm). The $^1$H NMR

spectra were recorded on a Bruker BioSpin (DPX-400) instrument and mass spectra were recorded on an Agilent 6430 LC-MS/MS spectrometer equipped with an electrospray ionization source (ESI). HPLC analyses were monitored by combined Shimadzu LC20A and Eckert & Ziegler HPLC Scan devices. Modular Lab-Pharm-Tracer synthesis device (Eckert & Ziegler Eurotope, Berlin, Germany) was used for labeling synthesis.

**Chemistry**

*Synthesis of precursor of [$^{18}$F]Flurpiridaz (7)*

*[2-(4-((1-tert-Butyl-5-chloro-6-oxo-1,6-dihydropyridazine-4-yloxy)methyl)benzyloxy)ethyl-4-methylbenzensulfonate] (6)*

Precursor **6** was synthesized according to the literature procedures with few changes (Purohit et al. 2008; Nagel 2014) Briefly, to a mixture of mucochloric acid (**1**) (1.18 g, 6.98 mmol) and Na$_2$CO$_3$ (0.33 g, 3.11 mmol) in 15 ml of distilled water was added *tert*-butylhydrazine hydrochloride (0.86 g, 6.90 mmol) in ice-water bath and reaction mixture was stirred for about 4 h. White precipitate was washed by water and dried under reduced vacuum after filtration. Then, 13.2 ml of benzene and acetic acid (1.86 g, 30,95 mmol) were added and reaction was kept at 40 °C for 4 h. Organic phase was extracted with 10 ml of water and washed by 5 ml of 1.25 M NaOH(aq), 5 ml of 5 M HCl(aq) and 10 ml of water respectively. 0.83 g of DCP (**2**) was obtained as an orange solid. 1.0 g of DCP (**2**) (4,53 mmol) was dissolved in 15 ml of dry DMF, 1,4-phenylene dimethanol (3.2 g, 23.16 mmol) and Cs$_2$CO$_3$ (6.0 g, 18.41 mmol) were slowly added to the solution and reaction was stirred at 68 °C under nitrogen atmosphere for about 6 h and allowed to be cooled down to room temperature. Crude product was extracted with CHCl$_3$/water several times and evaporated under vacuum. Residue was subjected to flash column chromatography (silica gel 40 g, EtOAc/Hexane 3:2) and 0.91 g of compound **3** was obtained as white solid. Then, 0.91 g of an alcoholic compound **3** was dissolved in 15 ml of freshly distilled dichloromethane and 0.14 ml of PBr$_3$ was slowly added to the solution. The reaction was carried out at room temperature for about 2 h under nitrogen atmosphere. Crude product was extracted with 30 ml of water and dried under vacuum. White solid product **4** was successfully obtained in a quantitative yield without further purification for next step. KO*t*Bu (0.28 g, 2.49 mmol) and 11.2 ml of ethylene glycol were stirred at room temperature under nitrogen atmosphere. Then, 0.95 g of bromide compound **4** dissolved in 8 ml of dry THF was added slowly into the reaction mixture and the reaction was stirred at 60 °C for overnight. After cooling to room temperature, THF was evaporated and residue was extracted with CHCl$_3$/water several times. Organic phase was evaporated under vacuum and residue was submitted to flash column chromatograpy (silica gel 40 g, EtOAc/Hexane 2:1) and 0.86 g of compound **5** was obtained as colorless oil in quantitative yield. Finally, to a mixture of 0.85 g of compound **5** and tosyl chloride (690 mg, 3.62 mmol) in 6 ml of dry dichloromethane, 0.64 ml of DIPEA and 4-(dimethylamino) pyridine (445 mg, 3.64 mmol) were added and reaction was carried out at room temperature for 2.5 h under nitrogen atmosphere. Dichloromethane was evaporated and crude product was directly subjected to flash column chromatograpy (silica gel 45 g, EtOAc/Hexane 2:1). 0.9 g of pure tosylate **6** (precursor of [$^{18}$F]Flurpiridaz) was obtained by recrystallisation in dichloromethane at+4 °C. Tosylate **6** was further purified through semipreparative HPLC for an accurate spectroscopic

characterization (Fig. 1). Anal. Calcd for $C_{25}H_{29}ClN_2O_6S$: C, 57.63; H, 5.61; Cl, 6.80; N, 5.38; S, 6.15. Found: C, 57.86; H, 5.84; Cl, 7.03; N, 5.66; S, 6.34.

^{1}H NMR ((CDCl$_3$, 400 MHz) $\delta$ (ppm)): 7,80 (d, $J=9.1$ Hz, 2H); 7,73 (s, 1H); 7,39 (d, $J=9.1$ Hz, 2H); 5,29 (s, 2H,); 4,49 (s, 2H,); 4,20–4,19 (m, 2H); 3,70–3,65 (m, 2H); 2,42 (s, 3H); 1,60 (s, 9H).

### *Purification of precursor 6*

### Characterization methods of precursor 6
### *HPLC analysis of precursor 6*
Chemical purity of the precursor was determined by HPLC analysis. Method parameters: Gradient flow: 0–15 min 40% B → 95% B,15–20 min 95% B (Phase A: H$_2$O (0.1% TFA), Phase B: ACN (0.1% TFA). Flow rate: 0.6 mL/min, UV: 320 nm, Column: ACE C18 3 μm, 3 mm × 50 mm, Injection volume: 20 μL, Precursor **6** RT: 11.5 min (Fig. 2a).

### *HR-MS analysis of precursor 6*
MS analysis was performed for precursor **6**. ESI–MS: calculated for $C_{25}H_{29}ClN_2O_6S$ [M]:521.0350, found 521.1133, [M + Na] + 543.1327, found 543.1319 (Fig. 2b).

### Radiochemistry
### *Synthesis of [^{18}F]Flurpiridaz (7)*
*Preliminary studies & synthesis of [^{19}F]Flurpiridaz (7) (Cold runs)    Materials* KF, Ethanol, and Acetonitrile were obtained from Sigma Aldrich. Kryptofix K2.2.2./K$_2$CO$_3$ (22 mg Kryptofix K2.2.2., 7 mg K$_2$CO$_3$, 300 μl acetonitrile and 300 μl pure water), TBA-HCO$_3$ (0.075 M) solution and QMA Cartridges were from ABX. Sep-Pak C18 Plus Light Cartridge was from Waters.
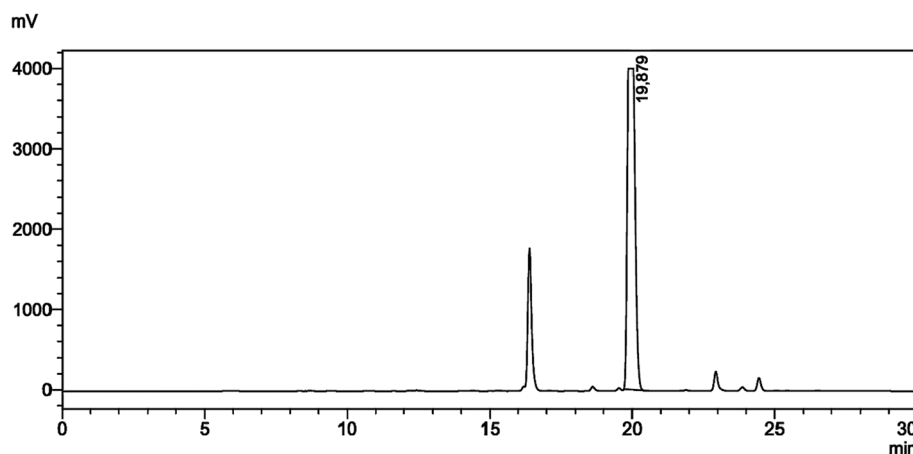


**Fig. 1** Purification (UV chromatogram) of precursor **6** (Method parameters: gradient flow; 0–10 min 40% B → 70% B, 10–20 min 70% B → 90% B, 20–25 min 90% B → 95% B, 25–30 min 95% B → 40% B (Phase A: H$_2$O, Phase B: ACN), flow rate: 4 mL/min, UV: 320 nm, Column: GL Inertsustain C18 5 μm, 10 × 250 mm, Injection volume: 5 mL, Precursor **6** RT: ~ 20 min.)
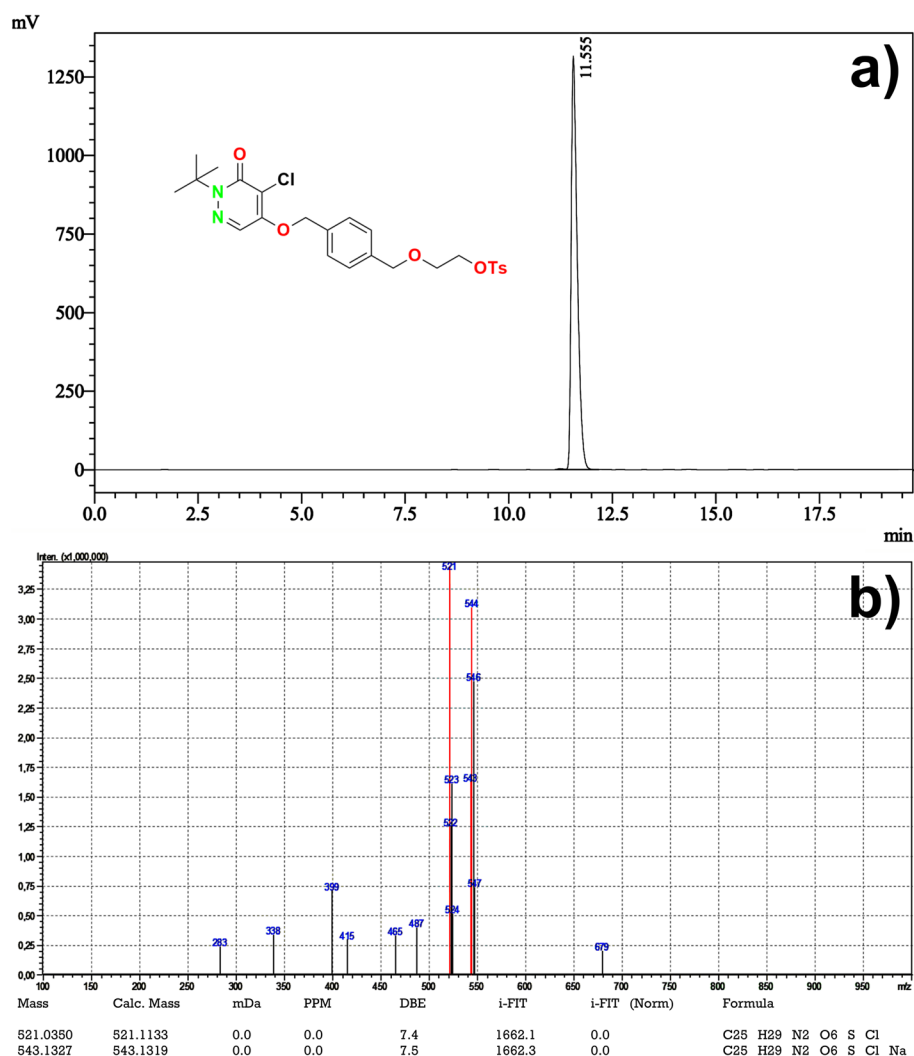
**Fig. 2** Chemical purity and identification (UV chromatogram) of precursor **6** (**a**), HR-MS spectrum of precursor **6** (**b**)
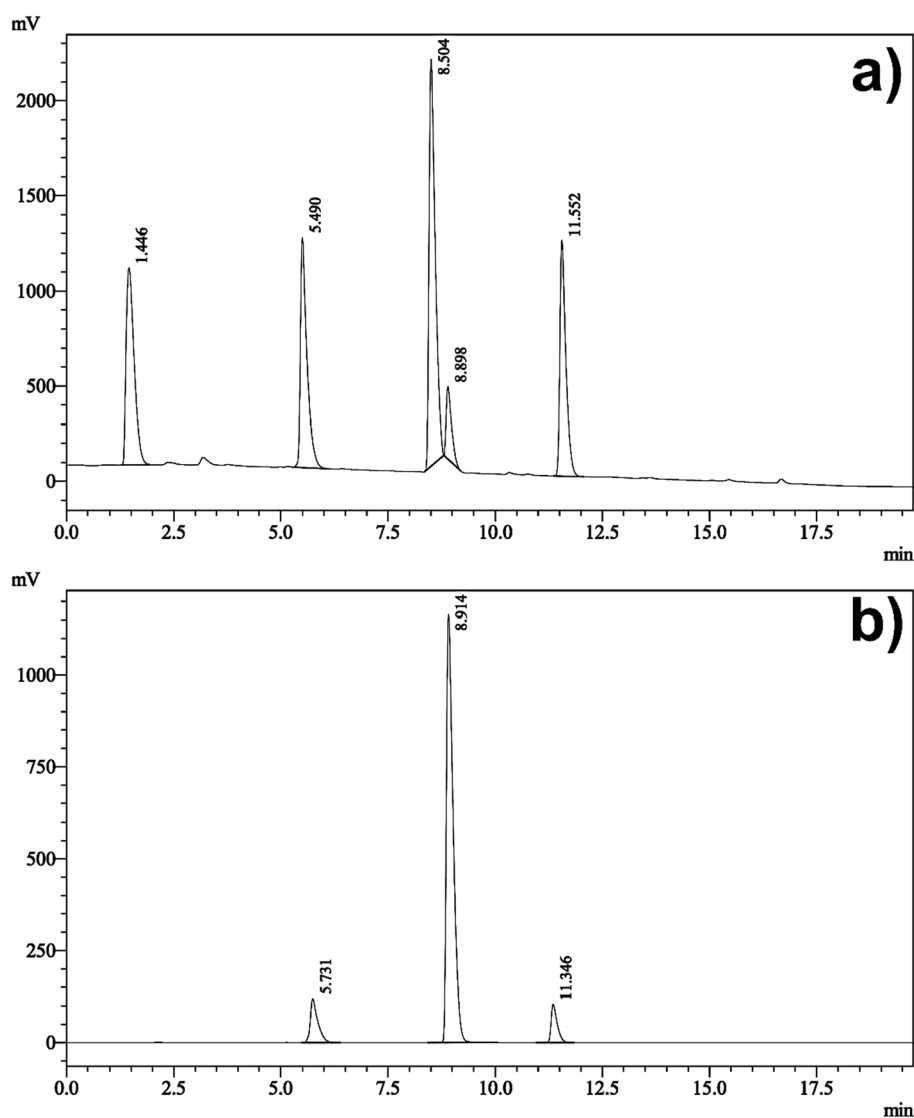
## Methods

Firstly, consecutive cold syntheses of [$^{19}$F]Flurpiridaz (**7**) were performed using stable isotope fluorine-19 and optimum reaction parameters were tried to be determined.

### Eluent solution-I (Kryptofix K2.2.2./K$_2$CO$_3$)

50 mg of KF was dissolved in 2 mL of ultrapure water and directly passed through the preconditioned QMA cartridge. The QMA cartridge was rinsed with 5 mL of ultrapure water and dried with N$_2$. [$^{19}$F]F trapped on the QMA cartridge was eluted into the reaction vial with 600 μL of Kryptofix K2.2.2./K$_2$CO$_3$ solution. Solvents in the reaction vial were removed at 100 °C, [$^{19}$F]F and Kryptofix K2.2.2./K$_2$CO$_3$ were dried gently. Then, 10 mg of precursor **6** dissolved in 2 mL of anhydrous acetonitrile was added to the reaction vial and the mixture was sealed and heated at 95 °C for 10 min. The reaction solution was diluted with 5 ml of ultrapure water and directly

passed through a preconditioned C-18 cartridge. C-18 cartridge was rinsed with 5 mL of ultrapure water and dried with air. Finally, C-18 cartridge was eluted with 5 mL of ethanol and transferred into the final product vial. The final product was diluted with 5 mL of ultrapure water (n = 3) and analyzed by HPLC (described in *HPLC analysis of precursor 6*) to determine its composition.

Chromatogram analysis indicated that four different separate peaks were observed. The unreacted precursor **6** was detected around 11.55 min. The other two peaks were detected between 8 and 9 min. Another major peak around 5.5 min was detected. It was concluded that the chemical yield of product **7** was low due to the majority of side-product formations (Fig. 3a).



**Fig. 3** Final product compositions (UV Chromatograms), Fluoride elution method-I (Kryptofix K2.2.2./$K_2CO_3$) (**a**), Fluoride elution method-II (TBA-$HCO_3$) (**b**)

### Eluent solution-II (TBA-HCO₃)

50 mg KF was dissolved in 2 mL of ultrapure water and directly passed through the preconditioned QMA cartridge. The QMA cartridge was rinsed with 5 mL of ultrapure and dried with $N_2$. [$^{19}$F]F trapped on the QMA cartridge was eluted into the reaction vial with 750 μL of TBA-HCO$_3$ solution (0.075 M). Solvents in the reaction vial were removed at 100 °C, [$^{19}$F]F and TBA-HCO$_3$ were dried gently. Then, 10 mg of precursor **6** dissolved in 2 mL of anhydrous acetonitrile was added to the reaction vial and the mixture was sealed and heated at 95 °C for 10 min. The reaction solution was diluted with 5 ml of ultrapure water and directly passed through a preconditioned C-18 cartridge. C-18 cartridge was rinsed with 5 mL of ultrapure water and dried with air. Finally, the C-18 cartridge was eluted with 5 mL of ethanol into the final product vial. The final product 7 was diluted with 5 mL of ultrapure water (n = 3) and analyzed by HPLC (described in *HPLC analysis of precursor 6*) to determine its composition.

A clear major peak around 9 min was detected which belongs to [$^{19}$F]Flurpiridaz (**7**). The unreacted precursor **6** was detected around 11.40 min. A possible side-product was detected around 5.5 min. as in the elution method-I, but there was relatively a small amount in the final product composition. Those analyses proved that the chemical yield is high, and the amount of side-product formation is quite low (Fig. 3b).

In this study, the substance obtained around the 9 min. was purified and isolated from the final product composition (Fig. 3b). HR-MS analysis was performed for the isolated concentrated pure substance (Fig. 4a) and it was clearly identified as [$^{19}$F]Flurpiridaz (**7**) (Fig. 4b). The second method was chosen as the elution method for the synthesis of [$^{18}$F]Flurpiridaz (**7**).

*Automated synthesis procedure of [$^{18}$F]Flurpiridaz (7)*    *Materials* Ethanol, *L*-ascorbic acid, and Acetonitrile were obtained from Sigma Aldrich. WFI, TBA-HCO$_3$-Solution, and QMA Cartridges were from ABX. O-18 Water was purchased from CMR. Disposable consumables, cassettes, and other accessories were obtained from Eckert & Ziegler. Other Sep-Pak Cartridges, tC18 Plus Long Cartridge, Sep-Pak Alumina N Plus Light Cartridge were from Waters.

### Method

We have developed an automated radiosynthesis procedure for [$^{18}$F]Flurpiridaz (**7**) on the ML PT synthesis device. Each step has been optimized with repetitive studies. The final product was isolated as a pure and sole product without further preparative HPLC purification process. Detailed synthesis steps such as [$^{18}$F]F trapping, [$^{18}$F]F elution, [$^{18}$F]F drying, radiolabeling, purification and product transfer were well described in Table 1.

### Quality control of [$^{18}$F]Flurpiridaz (7)

Radiochemical and chemical purity analyses of the final product [$^{18}$F]Flurpiridaz **(7)** were performed by Radio-HPLC (described in *HPLC analysis of precursor 6*) (Fig. 6). In addition, after the synthesis, the composition of the waste vial was analyzed by
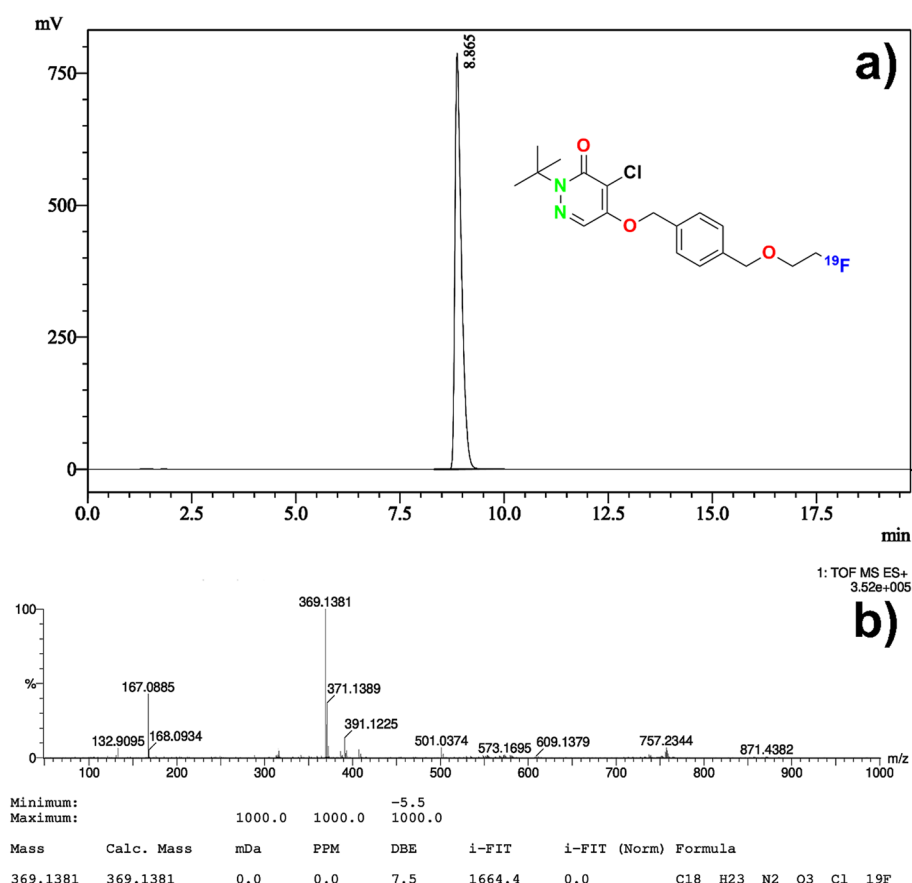
**Fig. 4** HPLC UV chromatogram and identification of [$^{19}$F]Flurpiridaz (**7**) (**a**), HR-MS analysis of [$^{19}$F]Flurpiridaz (**7**) (**b**)

Radio-HPLC. it was determined that free [$^{18}$F]F and other [$^{18}$F]F side products were clearly removed (Fig. 7).

## Results

Organic synthesis of precursor **6** was achieved in our laboratory with more than 99% chemical purity and a total yield of 35%. Structural analysis was confirmed by NMR, elemental analysis, and HR-MS which was consistent with previously published literature (Ahmed et al. 2020). Manually cold labeling experiments were afforded before the synthesis of [$^{18}$F]Flurpiridaz (**7**) starting from K$^{19}$F for optimization. HPLC UV and HR-MS results revealed that the nature of PTC was a dramatic effect on optimization and TBA-HCO$_3$ PTC increased the fluorination yield with a minimum amount of side product (Fig. 3b)**.** Parameters obtained by cold runs were tried to adapt ML PT synthesis module for hot runs (Tables 1, 2, 3). A fully automated radiosynthesis of [$^{18}$F]Flurpiridaz (**7**) was validated by three sequential syntheses. Table 3 and Fig. 5a presented that RCY was nearly 65% with more than 98% RCP. Table 4 summarizes the specifications of desired product 7 and entire results such as residual solvent, sterility, RCP, and BET are consistent with general radiopharmaceutical quality guidelines.

**Table 1** Radiosynthesis steps of [18F]Flurpiridaz (**7**)

| Step | | Reagents | Parameters |
|---|---|---|---|
| 1 | Trapping of [18F]F on the QMA cartridge | QMA cartridge, O-18 water | The irradiated O-18 water is vacuumed over the QMA cartridge into the O-18 recovery vial for 90 s |
| 2 | Drying of the QMA cartridge | QMA cartridge, $N_2$ | The QMA cartridge is dried with high flow $N_2$ for 90 s |
| 3 | Elution of [18F]F to the reaction vessel | 750 µL of TBA-$HCO_3$-Solution (0.075 M) | |
| 4 | Evaporation of solvents and drying process | | Solvents are evaporated under vacuum and low flow $N_2$ for 6 min |
| 5 | Transfer of precursor to the reaction vessel | 10 mg of precursor in 2 mL of anhydrous ACN | |
| 6 | Radiolabeling | | The reaction vessel is sealed and heated at 95 °C for 10 min |
| 7 | Loading of the reaction mixture into the purification cartridge tC18 | tC18 cartridge (pre-conditioned with 10 mL of ethanol, rinsed with ultrapure water, and dried with air) WFI | The reaction mixture is diluted with 6 mL of WFI and passed through tC18 The reaction vessel was rinsed a second time with 5 mL of WFI and passed through tC18 Finally, tC18 is rinsed with 10 mL of WFI and dried with $N_2$ [18F]Flurpiridaz, unlabeled precursor, and side products are trapped on the tC18 cartridge |
| 8 | Rinsing of tC18 cartridge with purification solution | 16 mL (40% ethanol/60% WFI, 50 mg/mL of Ascorbic Acid) | The more polar side-product is washed into the waste vial from tC18 Flow rate: 1 mL/min 20 min |
| 9 | Elution of [18F]Flurpiridaz into the 30 mL syringe from tC18 | 5 mL (50% ethanol-50% WFI) | [18F]Flurpiridaz is eluted into the 30 mL syringe Flow rate: 2 mL/min Almost entire of the more apolar unlabeled precursor remains in the tC18 cartridge, while [18F]Flurpiridaz is eluted by polarity difference |
| 10 | Dilution of [18F]Flurpiridaz in the 30 mL syringe | 20 mL of WFI | The precursor has no water solubility. The final product is diluted with 20 mL of WFI. In this way, Even a trace amount of precursor is precipitated |
| 11 | Transfer of the final product | The final vial content, 5 mLof WFI (1500 mg of Ascorbic Acid buffer pH: 6.7) The final purification cartridge: Sep-Pak Alumina N Plus Light Cartridge Two pieces of 0.2-micron sterilization filter | 25 mL of the final product [18F]Flurpiridaz is transferred to the final product vial, passing through the final purification cartridge and two sterilization filters Free [18F]F is removed by Alumina N cartridge. The trace amount of precursor precipitated is removed by two pieces of sterilization filter |

## Stability studies of [18F]Flurpiridaz (7)

After a successful validation of the synthesis of fluorinated product **7**, stability experiments were exhibited. Radiochemical purity analyzes were performed by Radio-HPLC at 2-h intervals from the end of the synthesizes (T0) for three separate productions. The final product [18F]Flurpiridaz (**7**) was observed for 12 h within the frame of this plan in room conditions. [18F]Flurpiridaz (**7**) remained within radiopharmaceutical quality

**Table 2** Description of the schematic synthesis diagram (Fig. 5)

| 1 | Low Flow N$_2$ (18–40 mL/min) | 12 | Chemical valve (open/close) |
|---|---|---|---|
| 2 | High Flow N$_2$ (300–500 mL/min) | 13 | Vacuum sensor |
| 3 | 750 µL of TBA-HCO$_3$-Solution (0.075 M) | 14 | Reactor, Heater |
| 4 | O-18/F-18 V-Vial | 15 | O-18 Recovery Vial (10 mL) |
| 5 | Sep-Pak Light QMA Cartridge | 16 | 10 mg of precursor in 2 mL of anhydrous ACN |
| 6 | 250 mL of WFI | 17 | Waste Vial |
| 7 | 5 mL (50% Ethanol—50% WFI) | 18 | 16 mL (40% ethanol / 60% WFI, 50 mg/mL of Ascorbic Acid) |
| 8 | Sep-Pak tC18 Plus Long Cartridge | 19 | Sep-Pak Alumina N Plus Light Cartridge |
| 9 | Radioactivity Detector | 20 | 0.2 Micron Sterilization Filters |
| 10 | Vacuum Pump | 21 | Final Product Vial (30 mL) + 5 mL 1500 mg Ascorbic Acid Buffer |
| 11 | Waste Bottle (250 mL) | 22 | 10 mL Syringe |
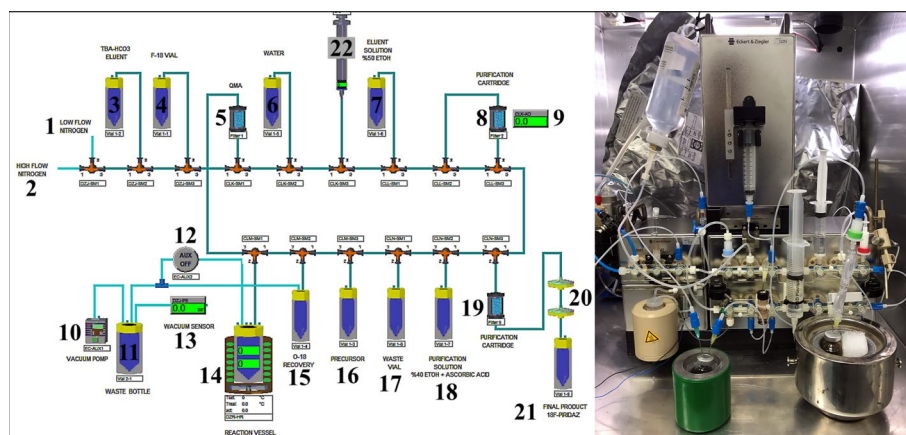


**Fig. 5** Schematic HMI diagram of the automated synthesis of [$^{18}$F]Flurpiridaz (**7**). And the photo of the cassette, reagents, and ML PT synthesizer

during this time. The entire analysis results, the average of the analysis results, and the RSD% are depicted in Fig. 8.

## Discussion

The radiolabeling procedure of radiopharmaceutical preparation is **a** critical case before clinical administration (De Decker and Turner 2011). Currently, majority of the radiopharmaceuticals are not commercially available and their "*in house preparation*" was mainly based on manual synthesis although manually process causes radiation exposure and contamination risk (Meyer et al. 2004). On the other hand, a fully automated preparation of radiopharmaceuticals provides standardization, minimal radiation exposure, validation, reproducibility, and high yield (Velikyan et al. 2015). Furthermore, a fully automated system facilitates a GMP-compliant production in clinical studies and disposable cassette systems are employed to prevent cross-contamination caused by tubing systems, which leads to sterile and highly pure radiolabeled compound. (Boschi et al. 2013).

Modular Lab-PharmTracer (ML PT) synthesizer is a fully user-defined system combined by activity detectors, valves, pressure sensor, pump, SPE cartridge and heater. All
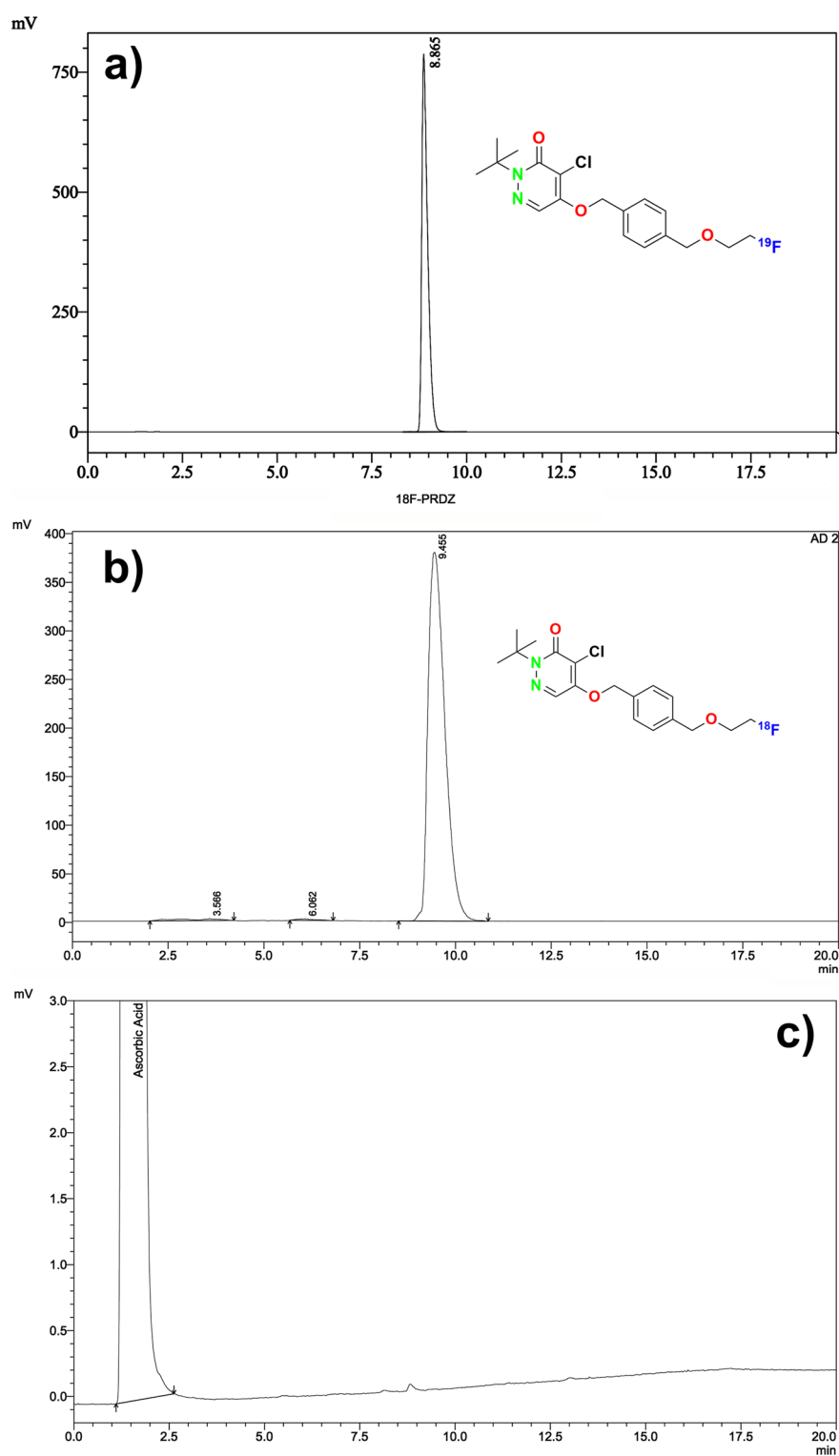
**Fig. 6** Radio-HPLC chromatogram and identification of [$^{18}$F]Flurpiridaz (**7**) (**b**), HPLC–UV chromatogram of [$^{18}$F]Flurpiridaz (**7**) (**c**), HPLC–UV chromatogram of [$^{19}$F]Flurpiridaz (**a**) (**7**)
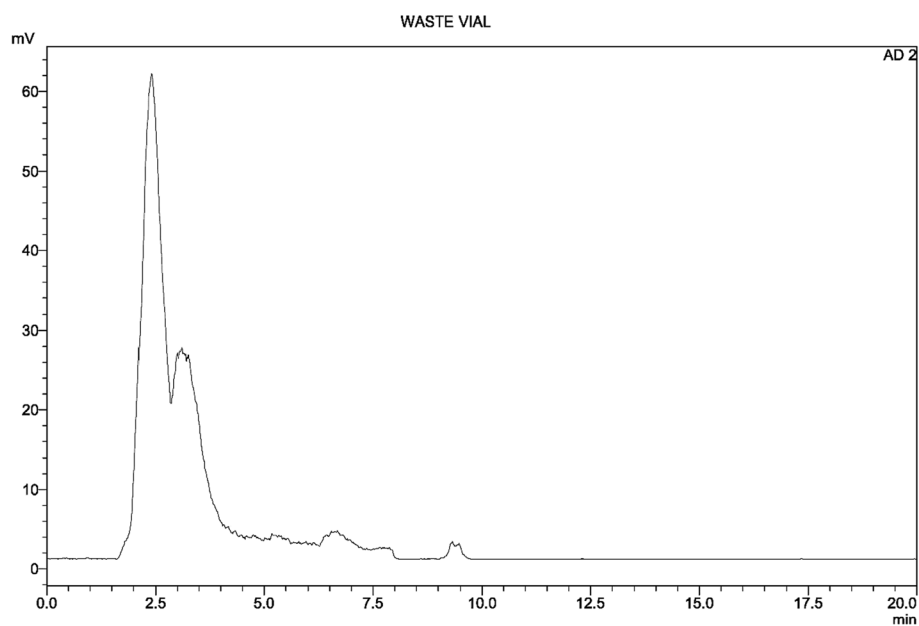
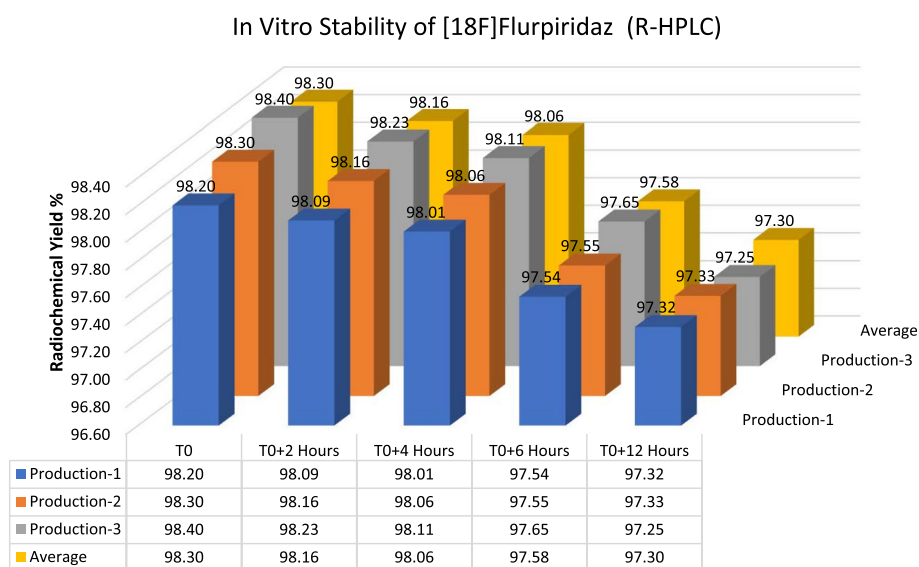**Fig. 7** Radio-HPLC chromatogram of the waste vial

**Table 3** General synthesis parameters (n = 3)

| Total duration of the synthesis | 110 min |
| --- | --- |
| Radiolabeling yield (Decay corrected) | 55–65% |
| Radiolabeling yield (Uncorrected) | 25–35% |
| Final product volume | 30 ml |

**Table 4** Final product specifications of [$^{18}$F]Flurpiridaz (**7**)

| Test | Method | Acceptance criteria | Average results |
| --- | --- | --- | --- |
| Appearance | Visual | Clear, Colorless, or Light Yellow | Clear, Colorless, or Light Yellow |
| pH | pH-Indicator Strip | 4.5–8.5 | 6–7 |
| Half-Life | Half-Life Measurement | 105–115 min | 109 min |
| Radiochemical Purity | Radio-HPLC | > 95% | 98.5% |
| Radionuclidic Purity | Gamma Spec | > 99.9% | > 99.9% |
| Precursor | HPLC | N.D | N.D |
| (TBA) | Spot Test | ≤ 2.6 mg/V | ≤ 2.6 mg/V |
| Ethanol | GC | ≤ 10% (h/h) | 8.2% (h/h) |
| Acetonitrile | GC | ≤ 4.1 mg / V | 0.04 mg / V |
| Ascorbic Acid | HPLC | ≤ 500 mg / V | 151 mg / V |
| BET | LAL | < 175 IU/V | < 175 IU/V |
| Sterility | Sterility Test | Sterile | Sterile |

*V: 3 mL

## In Vitro Stability of [18F]Flurpiridaz  (R-HPLC)



| | T0 | T0+2 Hours | T0+4 Hours | T0+6 Hours | T0+12 Hours |
|---|---|---|---|---|---|
| ■ Production-1 | 98.20 | 98.09 | 98.01 | 97.54 | 97.32 |
| ■ Production-2 | 98.30 | 98.16 | 98.06 | 97.55 | 97.33 |
| ■ Production-3 | 98.40 | 98.23 | 98.11 | 97.65 | 97.25 |
| ■ Average | 98.30 | 98.16 | 98.06 | 97.58 | 97.30 |

*%RSD    T0 = 0,1% , T0+2 = 0,07% , T0+4 = 0,05% , T0+6 = 0,06%, T0+12 = 0,04%*

**Fig. 8** Stability studies of [$^{18}$F]Flurpiridaz (**7**) (T0 = End of the synthesis, n = 3)
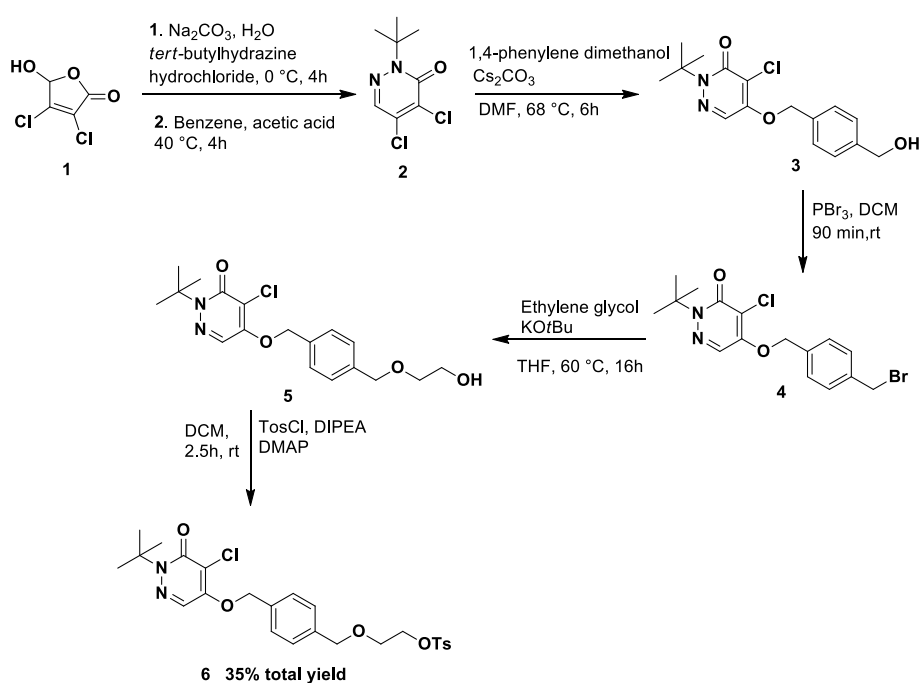


**Scheme 2** Synthesis of precursor (**6**) of [$^{18}$F]Flurpiridaz starting from mucochloric acid (**1**)

systems are controlled by an electric cabinet tool with an easy software program namely Modular-Lab. An appropriate system configuration enhances an efficient option for preparation of popular fluorine-18 based tracers such as [$^{18}$F]F-FES, [$^{18}$F]F-FDG, [$^{18}$F]F-PSMA-1007 and[$^{18}$F]F-FLT.

In light of the routine an automatically production of above fluorine-based compounds, we aimed to develop a fully automated synthesis of [$^{18}$F]Flurpiridaz **(7).** Firstly,
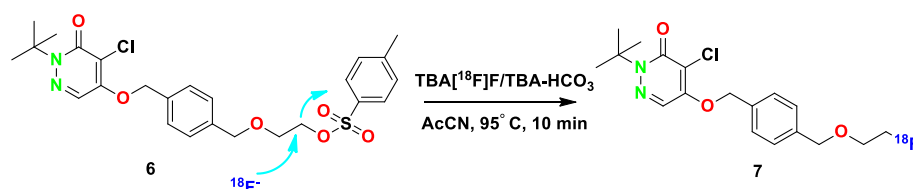
**Scheme 3** $S_N2$ reaction of precursor **6**

stepwise organic synthesis of flurpiridaz precursor (**6**) was achieved with a total yield of 35% and confirmed by NMR and HR-MS (Scheme 2).

After pure isolation of precursor **6**, optimized condition was aimed for radiolabeling of precursor **6**. In this work, amount of precursor, solvent type, reaction time and temperature were kept constant due to the previously published comprehensive study (Cesati et al. 2015). Firstly, cold experiments were tried to optimize reaction conditions without radioactive exposure. Stable isotope $[^{19}F]F$ was employed for nucleophilic substitution reaction. $^{19}$Flouride was trapped with QMA cartridge followed by elution with Kryptofix K2.2.2./$K_2CO_3$ as a phase transfer catalyst (PTC) which is widely used in $[^{18}F]$ flourine radiolabeling reactions. HPLC UV analysis (Fig. 3a) indicated that there was a dramatic increase of unexpected side products and a low amount of fluorination yield was observed. On the contrary, the chemical yield of fluorination increased with a minimum amount of side products in the presence of TBA-$HCO_3$ (Fig. 3b). The main reason for this result is that $HCO_3^-$ decreased the hydrolysis rate and increased the fluorination yield (Fig. 3a). Unfortunately, the basicity of $K_2CO_3$ caused the decomposition of the product and reduced fluorination yield. (Vavere et al. 2018). HR-MS and HPLC spectra identified relative quantity taking part in a reaction and precursor **6**, side products, and $[^{19}F]$Flurpiridaz **(7)** were well determined (Fig. 3,4).

After a sequential manually cold synthesis of $[^{19}F]$Flurpiridaz (**7**), an automated synthesis of radioactive fluorine compound was tried and each step was optimized with consecutive studies (Table 1). Fluorination of the precursor **6** is formed by $S_N2$ nucleophilic substitution reaction. The nucleophile $[^{18}F]$flouride attacks the backside of the carbon atom and the tosylate group was easily separated from the electrophilic carbon atom (Scheme 3). In general, use of polar aprotic solvents such as acetonitrile is very important for the activity of nucleophiles in $S_N2$ nucleophilic substitution reactions. Polar protic molecules such as water and ethanol make hydrogen bonds with nucleophiles, and they reduce the activity of nucleophiles and the yield of the labeling reaction. The cleavage of hydrogen bonds has to be afforded so that the nucleophile can attack to the electrophilic carbon. The fluoride ion, a weak nucleophile, is dramatically affected by the presence of impurities even in trace amounts during the labeling process and the reaction yield decreases. Therefore, evaporation of solvents and drying of TBA-$[^{18}F]$F & TBA-$HCO_3$ after QMA cartridge elution is a very critical process for desirable radiolabeling yield. The nature of the solvent is another critical parameter and anhydrous acetonitrile has to be used for high radiochemical yield.

Carefully spectral analyses showed that there were four main components in the post-reaction mixture; free $[^{18}F]$F, $[^{18}F]$Flurpiridaz **(7)**, non-radiolabeled precursor **6**, and one side-product (Fig. 3 **(b)**). In general, combined preparative HPLC system is frequently

utilized for the purification of the final fluorinated product in literature (Wang et al. 2020). Even this purification system has significant advantage for purification, this system is quite expensive, and a larger hot cell is required. For this reason, we aimed to design a simplified system for fast purification without using preparative HPLC. In our purification method, after the completion of radiolabeling, the reaction mixture was loaded onto the tC18 cartridge, and free fluorine and other polar impurities were transferred into the waste vial by water. Impurities which were slightly more polar than [$^{18}$F] Flurpiridaz (**7**) were washed into the waste vial by 16 ml of purification solution (40% ethanol/60% WFI, 50 mg/mL of ascorbic acid). At this step, the flow rate and ethanol concentration are another critical case for the exact separation of substances. The ascorbic acid in the solution was used to prevent radiolysis on the tC18 cartridge during this process. Then, the final product [$^{18}$F]Flurpiridaz (**7**) was eluted with 5 ml of solution (50% ethanol-50% WFI) into a 30 ml capacity injector with a certain flow rate. In this step, slightly non-polar precursor **6** also remained on the tC18 cartridge. Precursor **6** is not water-soluble, for this reason, an additional 20 ml of water was sent to the injector to precipitate precursor **6**, in case even trace amounts of precursor **6** are eluted with the final product. Finally, [$^{18}$F]Flurpiridaz (**7**) was successfully transferred to the final product vial through the alumina cartridge and two 0.2-micron sterilization filters. The alumina cartridge removed free [$^{18}$F]F residue, while the 0.2-micron filters prevented the precipitated precursor **6** from passing into the final product vial. The final product consists of [$^{18}$F]Flurpiridaz (**7**), 7–8% ethanol, and 50 mg/ml of ascorbic acid with a total volume of 30 ml. Ethanol and ascorbic acid are important for final product stabilization. [$^{18}$F]Flurpiridaz (**7**) was produced with decay-corrected 55–65% radiochemical yield, > 98% radiochemical purity, and in radiopharmaceutical quality (Tables 3, 4). Stability studies have demonstrated that the final product protected its stability with initial radiopharmaceutical quality for 12 h (Fig. 7).

## Conclusion

In conclusion, a fully automated synthesis of [$^{18}$F]Flurpiridaz (**7**) without further preparative HPLC purification on ML PT has been successfully described for the first time. Highly pure precursor **6** was synthesized with a total yield of 35% and well characterized by NMR and HR-MS. The carefully sequential set of cold trials were performed for optimization conditions before the hot reactions, and TBA-HCO$_3$ increased chemical yield with a minimum amount of side products. The evaluation of hot reaction records has proved that our automated synthesis method without further preparative HPLC purification enables the production of [18F]Flurpiridaz with > 98% radiochemical purity. All synthesis and purification steps were achieved without any manual interaction. Disposable cassette was employed to provide a limit of dose standard. The desirable radiopharmaceutical quality of the product was obtained without using a preparative HPLC system. Stability experiments were well exhibited and final specifications were recorded according to the acceptance criteria in Ph. Eur. regulations. This simplified system provided cost effectiveness and could lead to a practical diagnostic application for multicenter clinical trials.

## Abbreviations

| | |
|---|---|
| ACN | Acetonitrile |
| CAD | Coronary artery disease |
| CMR | Cardiac magnetic resonance |
| DCP | 2-(Tert-butyl)-4 5-Dichloropyridazin-3(2 h)-one |
| DCM | Dichloromethane |
| DIPEA | *N,N*-Diisopropylethylamine |
| DMF | Dimethyl Formamide |
| EtOAc | Ethyl acetate |
| HPLC | High performance liquid chromatography |
| HR MS | High resolution mass spectrometry |
| KF | Potassium fluoride |
| MC | Mitochondrial complex |
| ML PT | Modular Lab-PharmTracer |
| MPI | Myocardial perfusion imaging |
| NMR | Nuclear magnetic resonance |
| PET | Positron emission tomography |
| Ph Eur | European pharmacopeia |
| QC | Quality control |
| QMA | Quaternary methyl ammonium |
| SPECT | Single-photon emission computed tomography |
| TBA-HCO$_3$ | Tetrabutylammonium bicarbonate |
| TFA | Trifluoro acetic acid |
| THF | Tetrahydrofuran |
| TLC | Thin-layer chromatography |
| UV | Ultra violet |
| WFI | Water for injection |

## Declarations

**Ethical approval and consent to participate**
This study does not contain any clinical study.

**Consent for publication**
Not applicable.

**Competing interests**
No competing interests.

## References

Ahmed H, Haider A, Gisler L, Schibli R, Gebhard C, Ametamey SM. [18 F]Flurpiridaz: facile and improved precursor synthesis for this next-generation cardiac positron emission tomography imaging agent. ChemMedChem. 2020;15:1040–3. https://doi.org/10.1002/cmdc.202000085.

Autio A, Uotila S, Kiugel M, Kytö V, Liljenbäck H, Kudomi N, Oikonen V, Metsälä O, Helin S, Knuuti J, Saraste A, Roivainen A. $^{68}$Ga-DOTA chelate, a novel imaging agent for assessment of myocardial perfusion and infarction detection in a rodent model. J Nucl Cardiol. 2020;27:891–8. https://doi.org/10.1007/s12350-019-01752-6.

Bergmann SR, Herrero P, Markham J, et al. Noninvasive quantitation of myocardial perfusion in human subjects with O-15 labeled water and positron emission tomography. J Am Coll Cardiol. 1989;14:639–52.

Berman DS, Maddahi J, Tamarappoo BK, Czernin J, Taillefer R, Udelson JE, Gibson CM, Devine M, Lazewatsky J, Bhat G, Washburn D. Phase II safety and clinical comparison with single-photon emission computed tomography myocardial perfusion imaging for detection of coronary artery disease: flurpiridaz F18 positron emission tomography. J Am Coll Cardiol. 2013;61:469–77. https://doi.org/10.1016/j.jacc.2012.11.022.

Boschi S, Lodi F, Malizia C, Cicoria G, Marengo M. Automation synthesis modules review. Appl Radiat Isot. 2013;76:38–45.

Cesati RR, Cheesman EH, Lazewatsky J, Radeke HS, Mongeau E, Zdankiewicz DD, Devine M, Methods and apparatus for synthesizing imaging agents, and intermediates thereof. 2015 US8936777B2

Croteau E, Gascon S, Bentourkia M, Langlois R, Rousseau JA, Lecomte R, et al. [11C]Acetate rest-stress protocol to assess myocardial perfusion and oxygen consumption reserve in a model of congestive heart failure in rats. Nucl Med Biol. 2012;39:287–94.

Danad I, Raijmakers PG, Driessen RS, Leipsic J, Raju R, Naoum C, et al. Comparison of coronary CT angiography, SPECT, PET, and hybrid imaging for diagnosis of ischemic heart disease determined by fractional flow reserve. JAMA Cardiol. 2017;2:1100–7. https://doi.org/10.1001/jamacardio.2017.2471.

Davidson CQ, Phenix CP, Tai TC, Khaper N, Lees SJ. Searching for novel PET radiotracers: imaging cardiac perfusion, metabolism and inflammation. Am J Nucl Med Mol Imaging. 2018;8(3):200–27.

De Decker M, Turner JH. Automated module radiolabeling of peptides and antibodies with gallium-68, lutetium-177 and iodine-131. Cancer Biother Radiopharm. 2011;27:72–6. https://doi.org/10.1089/cbr.2011.1073.

Di Carli MF, Dorbala S, Meserve J, El Fakhri G, Sitek A, Moore SC. Clinical myocardial perfusion PET/CT. J Nucl Med. 2007;48:783–93.

Fowkes FG, Aboyans V, Fowkes FJ, McDermott MM, Sampson UK, Criqui MH. Peripheral artery disease: epidemiology and global perspectives. Nat Rev Cardiol. 2017;14:156–70. https://doi.org/10.1038/nrcardio.2016.179.

Huang SC, Williams BA, Krivokapich J, Araujo L, Phelps ME, Schelbert HR. Rabbit myocardial 82Rb kinetics and a compartmental model for blood flow estimation. Am J Physiol. 1989;256:1156–64.

Maddahi J, Lazewatsky J, Udelson JE, Berman DS, Beanlands RSB, Heller GV, Bateman TM, Knuuti J, Orlandi C. Phase-III clinical trial of fluorine-18 flurpiridaz positron emission tomography for evaluation of coronary artery disease. J Am Coll Cardiol. 2020;76(4):391–401. https://doi.org/10.1016/j.jacc.2020.05.063.

Meyer GJ, Mäcke H, Schuhmacher J, Knapp WH, Hofmann M. 68Ga-labelled DOTAderivatised peptide ligands. Eur J Nucl Med Mol Imaging. 2004;31:1097–104.

Nagel, V. Synthese und Evaluierung makrozyklischer $^{68}$Ga-MPI-Tracer auf Pyridaben-Basis. 2014. PhD Thesis. Mainz, Univ., Diss.

Purohit A, Radeke H, Azure M, Hanson K, Benetti R, Su F, Yalamanchili P, Yu M, Hayes M, Guaraldi M, Kagan M, Robinson S, Casebier D. J Med Chem. 2008;51:2954–70.

Schelbert HR, Phelps ME, Huang SC, et al. N-13 ammonia as an indicator of myocardial blood flow. Circulation. 1981;63:1259–72.

Wang M, Glick-Wilson BE, Zheng QH. Fully automated radiosynthesis and quality control of estrogen receptor targeting radiopharmaceutical 16α-[$^{18}$F]fluoroestradiol ([$^{18}$F]FES) for human breast cancer imaging. Appl Radiat Isot. 2020;160:109109. https://doi.org/10.1016/j.apradiso.2020.109109.

Wu MC, Chin KC, Lin KH, Chiu NT. Diagnostic efficacy of a lowdose 32-projection SPECT 99mTc-sestamibi myocardial perfusion imaging protocol in routine practice. Nucl Med Commun. 2009;30:140–7. https://doi.org/10.1097/MNM.0b013e328319e65f.

Velikyan I. 68Ga-based radiopharmaceuticals: production and application relationship. Molecules. 2015;20:12913–43.

## Publisher's Note

Springer Nature remains neutral with regard to jurisdictional claims in published maps and institutional affiliations.